FIN TWISTING AS A PASSIVE ENHANCEMENT TECHNIQUE FOR HIGH EFFICIENCY HEAT SINK DESIGN

by

Khayra MILOUDI[a], Imane ALIOUANE[a], Younes MENNI[a,b], Mustafa BAYRAM[c*], Omolayo M. IKUMAPAYI[d], Abiodun BAYODE[d], Tin Tin TING[e,f], and Salih OZER[g]

[a] Department of Mechanical Engineering, Institute of Technology, University Center Salhi Ahmed Naama (Ctr. Univ. Naama), Naama, Algeria
[b] College of Technical Engineering, National University of Science and Technology, Dhi Qar, Iraq
[c] Department of Computer Engineering, Biruni University, Istanbul, Turkey
[d] Department of Mechanical Engineering, Northwest University, Potchefstroom, South Africa
[e] Faculty of Data Science and Information Technology, INTI International University, Nilai, Malaysia
[f] School of Information Technology, UNITAR International University, Selangor, Malaysia
[g] Mus Alparslan University, Mechanical Engineering, Mus, Turkiye

Original scientific paper
https://doi.org/10.2298/TSCI2504179M

This investigation focuses on how longitudinally twisted fins influence the convective heat transfer and flow behavior within a 3-D aluminum heat sink. Using a finite element-based numerical model, the influence of fin twist angles, 10°, 15°, and 20°, was analyzed under laminar, incompressible, steady-state water flow conditions with Reynolds numbers ranging from 500-1500. The base of the heat sink is subjected to a constant heat flux of 20000 W/m², and the resulting flow and temperature fields were examined in detail. Velocity distributions revealed enhanced fluid mixing and vortex generation with increasing twist angle, while surface temperature contours and thermal gradients demonstrated improved heat removal performance. Quantitative metrics, including average heat transfer coefficients and Nusselt numbers, confirmed that the 20° twisted fins consistently outperformed the lower-angle configurations, especially at higher Reynolds numbers.

Key words*: passive cooling, thermal enhancement, fin geometry, heat sink, finite element simulation*

Introduction

In response to the growing thermal challenges in high power density electronics and compact energy systems, recent studies have explored a wide range of heat sink enhancements, focusing on innovative fin geometries, advanced materials, phase change integration, and data-driven optimization techniques. Geometric design remains central to performance improvements, with disk and helical fins demonstrated by Ashrafi *et al.* [1] for thermohydrodynamic enhancement in minichannels, while optimized pin-fin spacing in radial heat sinks [2], perforation shape optimization [3], tapered fin configurations [4], sinusoidal and rectangular fins in double-layer micro-channels [5], and streamwise variations in fin height [6] have shown considerable improvements in heat transfer and pressure drop characteristics. Choi *et al.* [7] ap-

* Corresponding author, e-mail: mustafabayram@biruni.edu.tr

plied ANN for multi-objective optimization of straight and forked fins in cylindrical heat sinks, while Yang *et al.* [8] employed topological optimization refine micro pin-fin configurations for high heat flux applications.

Fin configurational studies also include segmental plate-fin analysis [9], combinations of multiple pin-fin shapes [10], and groove geometry modifications around pin-fin perforations [11], all contributing to enhanced fluid mixing and reduced thermal resistance. In parallel, the integration of PCM has emerged as a viable method for transient thermal regulation. Researchers have demonstrated PCM-enhanced performance in finned heat sinks using plate-fins with hybrid nanoparticles [12], pin-fins [13], *T*-shaped fins [14], and plate-fin configurations filled with low-melting metals [15]. Further, numerical simulations of such systems [16] confirm their applicability for electronics operating under fluctuating thermal loads. Meanwhile, active and hybrid cooling mechanisms are gaining traction. Bilaskar *et al.* [17] investigated piezoelectric fan-induced flow over porous fin arrays, while Jatau *et al.* [18] proposed swirling jet impingement heat sinks, with and without internal pin-fins, for photovoltaic systems. Additional innovations include hybrid distributed jet/pin-fin micro-channel configurations [19], aluminum foam inserts in pin-fin arrays [20], and impinging jet micro-channels with inclined fins fabricated via additive manufacturing [21]. Flow boiling under sub-atmospheric pressures has also been explored in micro pin-fin arrays to exploit latent heat transfer effects [22]. To navigate the complex, multi-parameter design space, researchers have increasingly used numerical and machine learning tools [8].

Efficient thermal management is critical for high performance systems, especially in compact electronics. This study investigates a rectangular heat sink with twisted longitudinal fins, varying the twist angle from 10°-20° in 5° steps, to assess its impact on thermal performance. Using water as the working fluid under laminar flow, the finite element method is employed to analyze heat transfer and fluid-flow characteristics.

Physical and mathematical modelling

This investigation focuses on the thermal and fluid dynamic performance of a 3-D finned heat sink designed for electronic cooling applications, as illustrated in fig. 1. The configuration comprises a rectangular flow channel with dimensions of 0.15 m in length, 0.05 m in width, and 0.03 m in height, integrated with a solid aluminum base measuring 0.1 m × 0.05 m × 0.003 m. Uniformly affixed to this base are 24 aluminum twisted fins, each with dimensions of 0.0225 m × 0.02 m × $7.5 \cdot 10^{-4}$ m. These fins are arranged longitudinally and symmetrically, positioned 0.025 m from both the inlet and outlet edges. Three fin twist angles, 10°, 15°, and 20°, are considered to evaluate their influence on heat transfer enhancement.

The working fluid, water, is modeled as a laminar, incompressible, and steady-state flow. Boundary conditions at the inlet prescribe a uniform velocity profile corresponding to Reynolds numbers ranging from $5 \cdot 10^2$ to $1.5 \cdot 10^3$, with a constant inlet temperature of 20 °C. The outlet is maintained at atmospheric pressure. A uniform heat flux of $2 \cdot 10^4$ W/m² is imposed on the bottom surface of the finned base (0.1 m × 0.05 m × 0.003 m), while the remaining walls are treated as adiabatic. All solid and fluid interfaces enforce no-slip and impermeable boundary conditions. The thermal-hydraulic behavior is governed by the continuity, momentum, and energy equations, respectively:

$$\nabla \vec{u} = 0 \tag{1}$$

where $\vec{u} = (u, v, w)$ is the velocity vector in the *x*-, *y*-, and *z*-directions.

$$\rho\left(\vec{u}\nabla\right)\vec{u} = -\nabla p + \mu\nabla^2\vec{u} \tag{2}$$

where ρ is the density of water, μ – the dynamic viscosity, and p – the corresponds to the pressure field within the flow domain.

$$\rho C_p \left(\vec{u}\nabla \mathrm{T}\right) = k\nabla^2 T \tag{3}$$

where T is the temperature field, C_p – the specific heat capacity at constant pressure, and k – the thermal conductivity of the fluid.

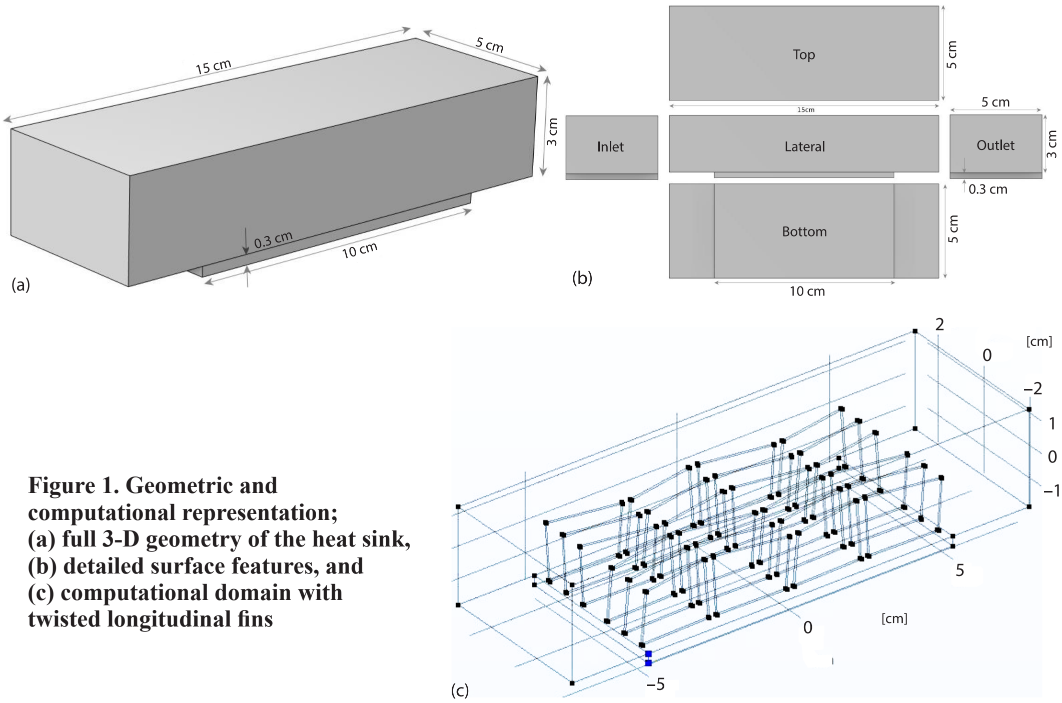

Figure 1. Geometric and computational representation; (a) full 3-D geometry of the heat sink, (b) detailed surface features, and (c) computational domain with twisted longitudinal fins

The computational domain is discretized using an unstructured mesh comprising a hybrid combination of tetrahedral, prismatic, pyramidal, and surface elements. The mesh consists of 1259985, 1260014, and 1264004 elements for the 10°, 15°, and 20° twisted fin configurations, respectively. Each mesh spans a total volume of 240 cm³. Minimum element qualities are 0.07227, 0.07334, and 0.07294 for the respective twist angles, while the corresponding average qualities are 0.6931, 0.6938, and 0.6940, values indicative of adequate mesh resolution and numerical stability across all cases. For validation, as depicted in fig. 2, the numerical results were compared with Chai *et al.* [23] for a rectangular straight micro-channel heat sink under identical geometric, thermal, and flow conditions. The comparison, based on wall temperature, shows strong agreement and confirms the accuracy of the present model.

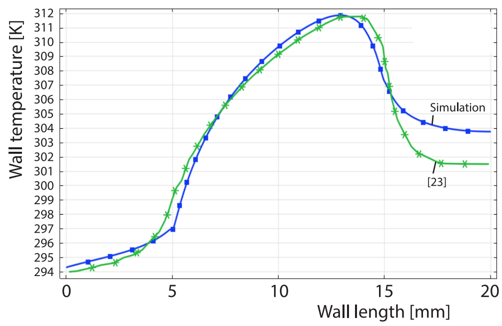

Figure 2. Model validation against reference

Results and analysis

Figure 3 illustrates the velocity magnitude contours at a Reynolds number of 500 for three different fin twist angles, 10°, 15°, and 20°. The results clearly demonstrate that increasing the twist angle leads to progressively more complex and disturbed flow fields. For the 10° configuration, the flow remains largely aligned with the main streamwise direction, exhibiting a relatively uniform velocity profile with minimal deviation or rotational components. This results in limited fluid mixing and weaker convective interactions near the fin surfaces. In contrast, the 15° twist angle introduces noticeable flow disruption, where mild vortices begin to form between adjacent fins, promoting transverse velocity components and moderate secondary flows. These changes enhance fluid mixing and begin to thin the boundary-layer near the heated surfaces, improving local convective heat transfer.

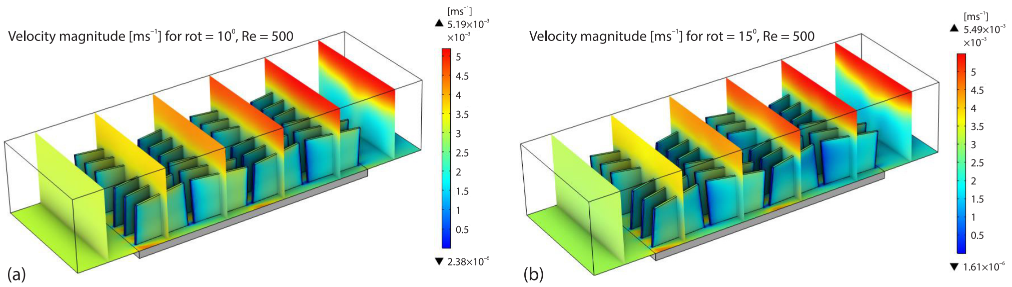

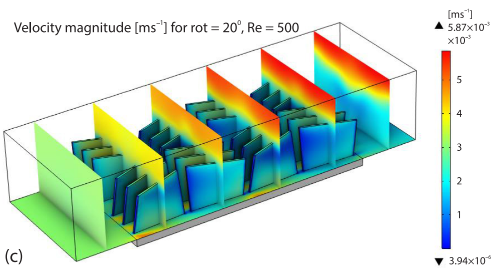

Figure 3. Velocity magnitude at Re = 500 for twist angles: (a) 10°, (b) 15°, and (c) 20°

At the highest twist angle of 20°, the flow becomes significantly more dynamic, with strong swirling motions and pronounced re-circulation zones developing between the fins. The induced vortices intensify lateral mixing and momentum diffusion across the channel, resulting in a more uniform velocity distribution and a substantial increase in the velocity gradients near the walls. This intensified flow agitation leads to a reduction in thermal boundary-layer thickness and enhances heat removal from the finned surfaces. Importantly, although the flow regime remains laminar at Re = 500, the geometric perturbations caused by twisted fins act as passive turbulence promoters, generating localized eddies that enhance convective transport without external energy input.

Figure 4 presents the temperature contours within the finned domain for the 20° twisted configuration at various Reynolds numbers, highlighting the influence of flow rate on heat removal effectiveness. As the Reynolds number increases from 500-1500, a significant reduction in temperature within the fluid domain is observed, particularly near the heated base. At Re = 500, the temperature field shows a thicker thermal boundary-layer and higher fluid temperatures adjacent to the finned surfaces, indicating limited convective transport and a greater reliance on conduction. The thermal gradient is concentrated near the base, and the heat dissipation into the fluid is relatively weak due to the low fluid momentum. When the Reynolds number rises to 1000, the thermal boundary-layer becomes noticeably thinner, and cooler fluid penetrates deeper between the fins. This behavior reflects improved convective mixing and more efficient thermal exchange between the solid and fluid phases. At Re = 1500, the temperature contours show even more extensive cooling, with the heated region near the base greatly diminished in thickness. The fluid motion is stronger and more rotational, driven by both the fin-induced swirling effects and the increased inertial forces associated with higher Reynolds number. This leads to a more uniform temperature field, reduced hot spots, and enhanced energy removal from the base. Additionally, the increased Reynolds number shortens the thermal residence time but is counterbalanced by the stronger convective currents, which sustain high heat transfer rates.

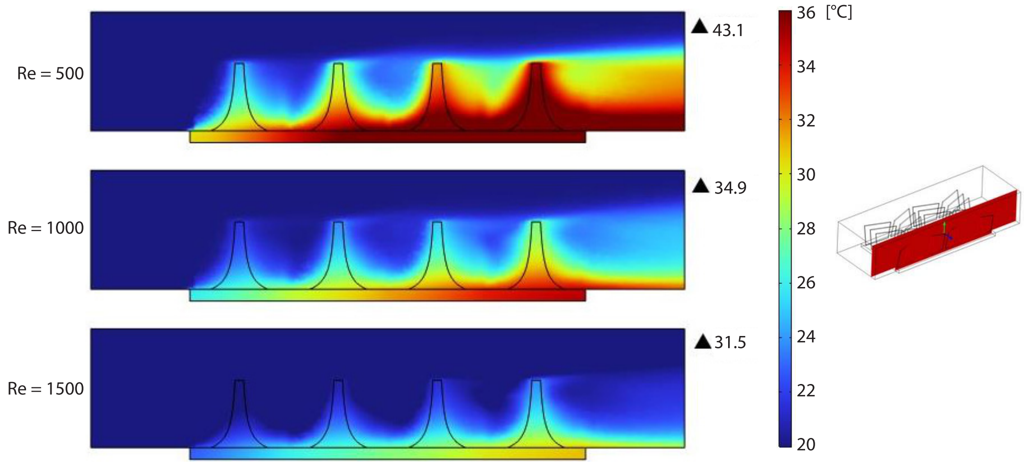

Figure 4. Influence of Reynolds number on temperature fields for a 20° twisted fin configuration

Figure 5 presents the surface temperature distribution of the finned base for different twist angles at Reynolds numbers of 500 and 1500, highlighting the thermal performance at the solid–fluid interface. At Re = 500, the surface temperature remains relatively high across all configurations due to the limited convective capacity of the low-velocity flow. Among the three twist angles, the 20° configuration consistently achieves the lowest surface temperatures, indicating enhanced convective heat transfer driven by stronger fluid mixing and more vigorous circulation within the finned region. In contrast, the 10° fins yield higher base temperatures, particularly near fin roots and corners, where stagnant zones develop due to weaker secondary flows. The 15° case shows moderate improvement but does not match the cooling efficiency achieved with the 20° fins. As the Reynolds number increases to 1500, a substantial reduction in

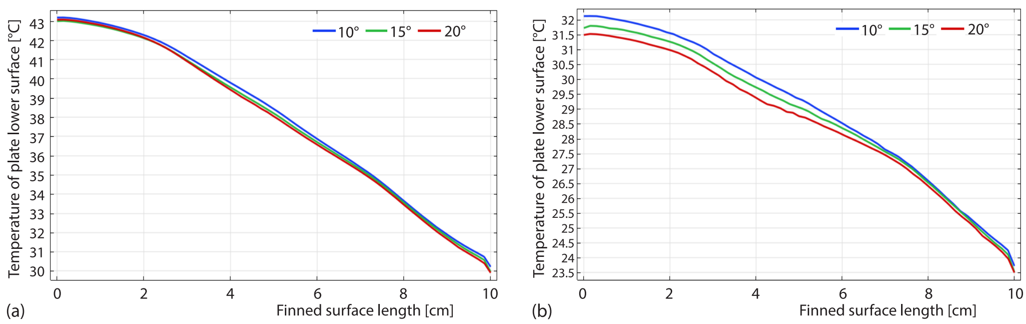

Figure 5. Surface thermal response at twist angles for (a) Re = 500 and (b) Re = 1500

surface temperature is observed for all configurations, with more uniform temperature distributions developing across the base. The 20° fins maintain superior performance, further lowering temperatures and effectively minimizing thermal hotspots. This improvement is attributed to the synergistic effect of increased twist and flow momentum, which together enhance boundary-layer disruption and promote deeper fluid penetration between the fins. The resulting increase in convective surface interaction improves local heat removal and ensures more efficient utilization of the available surface area.

Figure 6 presents the average heat transfer coefficients for fin twist angles of 10°, 15°, and 20° across Reynolds numbers of 500, 1000, and 1500, revealing the combined influence of geometry and flow conditions on convective performance. At Re = 500, all three configurations exhibit relatively similar values, ranging from 7161.2-7223.5 W/m²K, with only a slight increase observed as the twist angle increases. This marginal difference reflects the limited momentum of the low-speed flow, where fin-induced mixing is insufficient to substantially alter boundary-layer behavior. However, as the Reynolds number increases to 1000, the thermal enhancement becomes more noticeable. The 20° twisted fins achieve a heat transfer coefficient of 15633 W/m²K, outperforming the 10° and 15° cases by approximately 5.2% and 3.7%, respectively. This improvement stems from the more intense swirling motion and enhanced fluid-surface interaction resulting from the increased twist, which promotes better thermal boundary-layer disruption. At Re = 1500, this trend intensifies further: the 20° fins reach a heat transfer coefficient of 24388 W/m²K, showing a clear advantage over the 10° and 15° fins by about 7.7% and 5% , respectively. The superior performance at higher Reynolds numbers is attributed to the synergistic effect of stronger inertial forces and fin-induced rotational flows, which together generate higher convective activity and more efficient heat dissipation.

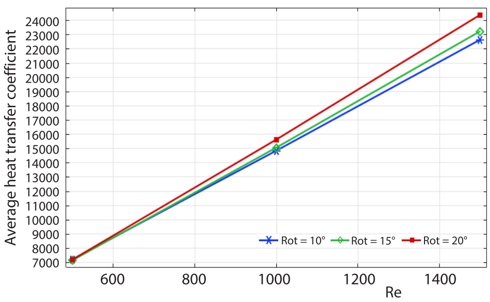

Figure 6. Effect of fin twist angle and Reynolds number on the average heat transfer coefficient

Figure 7 illustrates the average Nusselt numbers for different fin twist angles and Reynolds numbers, highlighting key trends in convective heat transfer enhancement. At low Reynolds number, Nusselt number values are closely spaced (19.418-19.635), indicating limited thermal improvement due to weak flow-induced mixing. As Reynolds number increases, especially at 1000 and above, the impact of fin twisting becomes more pronounced. The 20° twist configuration achieves a Nusselt number of 27.580 at high Reynolds number, marking a 5.25% improvement over the 10° case. These results confirm that higher twist angles more effectively disrupt the boundary-layer and enhance heat transfer, particularly under stronger inertial flow conditions.

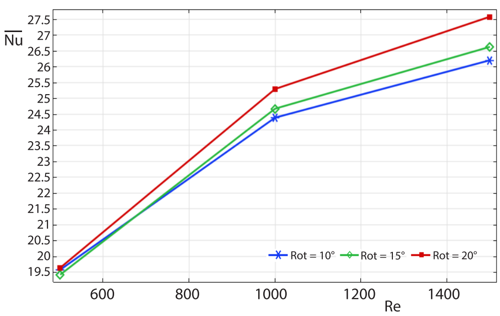

Figure 7. Influence of fin twist angle and flow conditions on average Nusselt number

Conclusion

This study numerically analyzed a 3-D aluminum heat sink with twisted longitudinal fins under laminar water flow, focusing on twist angle and Reynolds number effects. Increasing the twist angle from 10-20° significantly enhanced heat transfer by intensifying secondary flows and disrupting the thermal boundary-layer, with improvements more evident at higher Reynolds number. The 20° twist consistently achieved the highest heat transfer coefficients and Nusselt numbers, while also improving surface temperature uniformity and reducing hotspots. These findings highlight twisted fins as an effective passive cooling strategy for compact, high performance electronic systems.

References

[1] Ashrafi, M. M. A., *et a*l., Innovative Disk and Helical Fin Designs for Thermohydrodynamic Enhancement of Minichannel Heat Sinks, *Case Studies in Thermal Engineering*, *73* (2025), 106613
[2] Tripathy, T. L., Dash, S. K., Optimum pin-fin spacing of branching radial heat sinks under natural-convection for LED cooling, *International Journal of Thermal Sciences*, *215* (2025), 109973
[3] Rajan, A., *et al.*, Optimisation of the Heat Sink's Fin Perforation Shape Using Numerical Methods for Natural and Forced Convection in Electronic Cooling Applications, *Progress in Engineering Science*, *2* (2025), 100084
[4] Alam, *et al.*, Optimization of Tapered Pin Fins for Enhanced Heat Transfer in Micro-Channel Heat Sink, *International Journal of Thermal Sciences*, *214* (2025), 109889
[5] Maheswari, A., *et al*., . Thermo-Hydraulic Performance in Modified Double-Layer Micro-Channel Heat Sinks Designs: Optimization of Sinusoidal and Rectangular Fin Configurations for Enhanced Fluid Mixing And Heat Transfer Efficienc, *International Journal of Thermal Sciences*, *215* (2025), 109967
[6] Kumar, R., Pandey, M., Numerical Analysis of Heat Transfer and Fluid-Flow Characteristics of Micro-Channel Heat Sinks with Streamwise Variation of Fin Height, *International Communications in Heat and Mass Transfer*, *163* (2025), 108706
[7] Choi, J., *et al*., Multi-Objective Optimization of a Cylindrical Heat Sink With Straight and Forked Fins Using Artificial Neural Network (ANN), *International Communications in Heat and Mass Transfer*, *165* (2025), 109082
[8] Yang, H., *et al*., Topological Optimization Design of Micro-Pin Fin Heat Sinks for High Heat Flux Cooling Application, *International Journal of Thermal Sciences*, *218* (2025), 110102
[9] Dadda, *et al*., CFD-ANN-based model for parametric analysis of segmented plate-fin heat sinks: Exploring heat transfer and pressure drop trade-offs, *International Journal of Thermal Sciences*, *218* (2025), 110109
[10] Madi, K., *et al.*, Enhanced Thermal Management in Microelectronic Cooling: A Study on Pairing Multiple Pin-Fin Shapes in Micro-Channel Heat Sinks, *International Journal of Thermofluids*, *28* (2025), 101283
[11] Wongcharoen, A., *et al*., Effects of Groove Geometry Around Pin-Fin Perforation Circumference on Thermohydraulic Behavior of Pin-Fin Heat Sinks under Turbulent Flow, *Case Studies in Thermal Engineering*, *71* (2025), 106184
[12] Arshad, A., *et al*., Enhanced heat transfer of PCM-Based Heat Sink Augmented with Plate-Fins and Hybrid Nanoparticles for Electronics Cooling, *International Journal of Thermal Sciences*, *218* (2025), 110107
[13] Zhang, D. X., *et al*., Thermal Control Performance of a Novel PCM-Based Pin fin Hybrid Heat Sink, *Journal of Energy Storage*, *131* (2025), 117630
[14] Chuang, C. A., Chueh, C. C., Enhanced Thermal Efficiency of PCM-Integrated heat sinks: Insights into *T*-shaped Fins and PCM – Air Interface morphology, *Journal of Energy Storage*, *128* (2025), 117201
[15] Yang, Y. X., *et al*., Numerical Simulation of Plate Fin Heat Sinks Filled with Low-Melting Metal PCM for High Heat Flux Chips, *Journal of Energy Storage*, *131* (2025), 117524
[16] Han, F., Numerical Investigations on the Heat Transfer Characteristics of Pin-Fin Heat Sink for Power Converters in More Electric Aircraft, *International Communications in Heat and Mass Transfer*, *164* (2025), 108866
[17] Bilaskar, R., *et al.*, Heat Transfer and Acoustics Investigation of A Piezoelectric Fan-Porous Finned Heat Sink System in the Presence of Channel Flow, *Thermal Science and Engineering Progress*, *65* (2025), 103851
[18] Jatau, T., *et al*., Novel Design of Swirling Jet Impingement Heat Sink With and Without Internal Pin-Fins for Thermal Management of High-Concentrator Photovoltaic Systems, *Renewable Energy*, *243* (2025),

122614
[19] Liu, J., *et al*., Enhanced Flow Boiling Heat Transfer in Embedded Hybrid Distributed Jet/Pin-Fin Micro-Channel Heat Sink, *Experimental Thermal and Fluid Science*, *168* (2025), 111508
[20] Bayrak, F. T., *et al*., The Influence of Slotted Solid Cylindrical Fin with Aluminum Foam Insert on the Thermal and Hydraulic Characteristics of Air-Cooled Pin-Fin Heat Sink, *International Communications in Heat and Mass Transfer*, *162* (2025), 108595
[21] Liu, L., *et al*., Thermal-Dynamic Study on the Novel Designed Double-Layer Impinging Jet Micro-Channel Heat Sinks With Horizontal and Inclined Fins Verified by Additive Manufacturing Technology, *Applied Thermal Engineering*, *269* (2025), 126185
[22] Hu, W., *et al*., Flow Boiling of Water in a Micro Pin-Fin Heat Sink at Sub-Atmospheric Pressure, *International Journal of Thermal Sciences*, *215* (2025), 110032
[23] Chai, L., *et al*., Heat Transfer Enhancement in Micro-Channel Heat Sinks with Periodic Expansion-Constriction Cross-Sections, *International Journal of Heat and Mass Transfer*, *62* (2013), July, pp. 741-751

Paper submitted: February 14, 2025
Paper revised: June 15, 2025
Paper accepted: July 23, 2025